

## Simulation Analysis of the Retinal Conformational Equilibrium in Dark-Adapted Bacteriorhodopsin

Jérôme Baudry,\* Serge Crouzy,# Benoît Roux,§ and Jeremy C. Smith\*<sup>¶</sup>

\*Section de Biophysique des Protéines et des Membranes, DBCM, CEA-Saclay, 91191 Gif-sur-Yvette Cedex, France; #Biologie Moléculaire et Cellulaire, DBMS CEA-Grenoble, 38054 Grenoble Cedex 9, France; §Département de Chimie, Université de Montréal, Montréal H3C 3J7, Canada; and <sup>¶</sup>Lehrstuhl für Biocomputing, IWR, Universität Heidelberg, 69120 Heidelberg, Germany

**ABSTRACT** In dark-adapted bacteriorhodopsin (bR) the retinal moiety populates two conformers: all-*trans* and (13,15)*cis*. Here we examine factors influencing the thermodynamic equilibrium and conformational transition between the two forms, using molecular mechanics and dynamics calculations. Adiabatic potential energy mapping indicates that whereas the twofold intrinsic torsional potentials of the C13=C14 and C15=N16 double bonds favor a sequential torsional pathway, the protein environment favors a concerted, bicycle-pedal mechanism. Which of these two pathways will actually occur in bR depends on the as yet unknown relative weight of the intrinsic and environmental effects. The free energy difference between the conformers was computed for wild-type and modified bR, using molecular dynamics simulation. In the wild-type protein the free energy of the (13,15)*cis* retinal form is calculated to be 1.1 kcal/mol lower than the all-*trans* retinal form, a value within  $\sim k_B T$  of experiment. In contrast, in isolated retinal the free energy of the all-*trans* state is calculated to be 2.1 kcal/mol lower than (13,15)*cis*. The free energy differences are similar to the adiabatic potential energy differences in the various systems examined, consistent with an essentially enthalpic origin. The stabilization of the (13,15)*cis* form in bR relative to the isolated retinal molecule is found to originate from improved protein-protein interactions. Removing internal water molecules near the Schiff base strongly stabilizes the (13,15)*cis* form, whereas a double mutation that removes negative charges in the retinal pocket (Asp<sup>85</sup> to Ala; Asp<sup>212</sup> to Ala) has the opposite effect.

### INTRODUCTION

Bacteriorhodopsin (bR) is the light-driven proton pump protein from the purple membrane of the bacterium *Halobacterium salinarium* (Oesterhelt and Stoeckenius, 1971). BR contains a retinal chromophore (see Fig. 1) covalently linked to Lys<sup>216</sup> via a protonated Schiff base. After absorption by bR of a 568-nm photon, the retinal undergoes a conformational change that leads to the transfer of a proton from the intracellular to the extracellular side of the membrane.

The light-adapted form of bR contains  $\sim 100\%$  all-*trans* retinal (in which all of the double bonds of the polyene are in the *trans* conformation). However, after several minutes in the dark, the protein reaches a dark-adapted state. This state has an absorption maximum at 558 nm and contains a mixture of two isomers of retinal (Harbison et al., 1984): all-*trans* and C13=C14 *cis*, C15=N16 *syn*, abbreviated here to (13,15)*cis*, (in which the dihedral angles C13=C14 and C15=N16 are both *cis*). The two corresponding forms of the protein, denoted bR<sub>568</sub> (all-*trans* retinal) and bR<sub>548</sub> ((13,15)*cis* retinal), have absorption maxima at 568 nm and

548 nm, respectively. Experiments on retinal extraction followed by high-pressure liquid chromatography have led to the suggestion that the bR<sub>548</sub> form populates about two-thirds of the total in the dark-adapted state (Scherrer et al., 1989; Song et al., 1995). The population ratio is modified by changes in temperature, pH, amino acid sequence of bR (Song et al., 1995), and pressure (Schulte and Bradley, 1995; Schulte et al., 1995). The retinal isomer ratio has also been determined on membranes treated with Triton X-100, a detergent that produces monomers of bR (Massote and Aghion, 1991), giving a population of 71% of bR<sub>548</sub> at 277 K (Scherrer et al., 1989). The relative populations of the two forms in the dark-adapted bR suggest that the difference in their free energies is  $\leq k_B T$  (where  $k_B$  is the Boltzmann constant and  $T$  is the temperature).

Important questions remain concerning dark-adapted bR, including the isomerization pathway from (all-*trans*) to (13,15)*cis* retinal, and the factors influencing the conformational equilibrium. Calculations based on atomic models can be used to address these questions. Molecular dynamics simulations have been performed to examine other aspects of bR, including steps along the photocycle (Humphrey et al., 1994, 1998; Xu et al., 1995, 1996; Edholm et al., 1995; Ben-Nun et al., 1998; Hermone and Kuczera, 1998). A simulation model of bR<sub>568</sub> has been presented (Ferrand et al., 1993b) and the thermodynamic stability of internal water molecules examined (Nina et al., 1993, 1995; Roux et al., 1996). Recently a structure was proposed for (13,15)*cis* bR, and its photocycle was simulated (Logunov et al., 1995). The results of this study provided insight into why the photocycle of (13,15)*cis* does not pump protons; the

Received for publication 4 September 1998 and in final form 6 January 1999.

Address reprint requests to Dr. Jeremy C. Smith, Lehrstuhl für Biocomputing, IWR, Universität Heidelberg, Im Neuenheimer Feld 368, 69120 Heidelberg, Germany. Tel.: 49-6221-54-8857; Fax: 49-6221-54-8850; E-mail: biocomputing@iwr.uni-heidelberg.de.

Dr. Baudry's present address is Theoretical Biophysics Group, The Beckman Institute for Advanced Science and Technology, University of Illinois at Urbana-Champaign, 405 N. Matthews, Urbana, IL 61801.

© 1999 by the Biophysical Society

0006-3495/99/04/1909/09 \$2.00

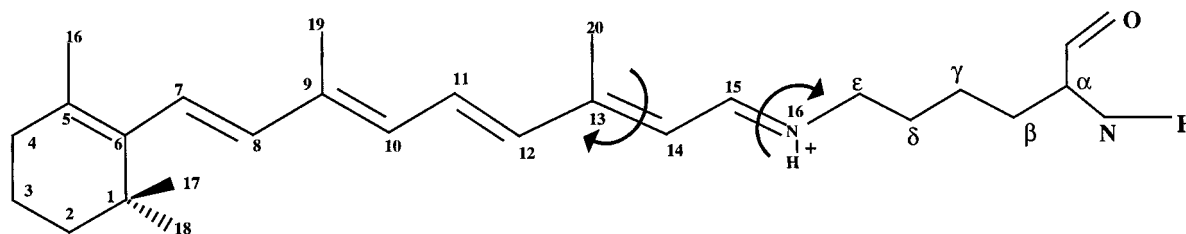


FIGURE 1 Retinal bonded to Lys<sup>216</sup>. Arrows indicate the isomerized dihedral angles in the dark-adapted state.

Schiff base nitrogen points to the intracellular side after photoisomerization of retinal. The isomerization pathway and the dark-adaptation kinetics have also been examined (Logunov and Schulten, 1996).

In preliminary work on the dark-adapted conformational equilibrium, we used quantum chemical calculations and free energy simulations to examine the relative energies of the all-*trans* and (13,15)*cis* conformers of isolated retinal molecules, subject to harmonic restraints designed such that the conformational flexibility of the chromophore in the protein was approximately reproduced (Baudry et al., 1997). The all-*trans* form was found to be  $\sim 2.1$  kcal/mol lower in free energy than the (13,15)*cis* form. This is in contrast to the higher proportion of the (13,15)*cis* form observed in dark-adapted bR, suggesting that the equilibrium in bR is significantly affected by interactions between the protein and the retinal and/or the effect of the retinal on the protein-protein interactions. Here the dark-adaptation pathway for the conformational change from all-*trans* to (13,15)*cis* retinal is examined. The (13,15)*cis*-all-*trans* free energy difference is calculated using umbrella sampling with the Weighted Histogram Analysis Method (Kumar et al., 1992). Agreement with the experiment is found to within  $\sim k_B T$ . Calculations on modified bR allow factors strongly influencing the conformational equilibrium to be identified.

## METHODS

### Molecular mechanics force field

The CHARMM (Brooks et al., 1983) potential energy function was employed in all of the molecular mechanics and dynamics calculations and has the following form:

$$\begin{aligned}
 V(\mathbf{R}) = & \sum_{\text{bonds}} k_b (b - b_0)^2 + \sum_{\text{angles}} k_\theta (\theta - \theta_0)^2 \\
 & + \sum_{\text{Urey-Bradley}} k_u (u - u_0)^2 \\
 & + \sum_{\text{impropers}} k_\omega (\omega - \omega_0)^2 \\
 & + \sum_{\text{dihedrals}} k_\phi (1 + \cos[n\phi - \delta]) \\
 & + \sum_{i,j} 4\epsilon_{ij} \left[ \left( \frac{\sigma_{ij}}{r_{ij}} \right)^{12} - \left( \frac{\sigma_{ij}}{r_{ij}} \right)^6 \right] \\
 & + \sum_{i,j} \frac{1}{4\pi\epsilon_0} \frac{q_i q_j}{r_{ij}}
 \end{aligned} \quad (1)$$

The potential energy function includes bonded interactions, comprising bond stretches, bond angle bends and dihedral angle contributions, and nonbonded interactions between pairs ( $i, j$ ) of atoms. In Eq. 1,  $b$ ,  $u$ ,  $\theta$ , and  $\omega$  are the bond lengths, Urey-Bradley 1:3 distances, bond angles, and improper dihedral angles in any given configuration, and  $b_0$ ,  $u_0$ ,  $\theta_0$ , and  $\omega_0$  are the reference values for these properties. The associated force constants are  $k_b$ ,  $k_u$ ,  $k_\theta$ , and  $k_\omega$ . The improper dihedral contributions are used to represent out-of-plane deformations of  $sp^2$  groups. For the intrinsic dihedral angles  $\phi$ ,  $k_\phi$  is the force constant,  $n$  is the symmetry of the rotor (e.g., 3 for a methyl group), and  $\delta$  is the phase angle.

The nonbonded interactions are included between pairs  $i, j$  of atoms on different molecules and on the same molecules separated by three or more bonds. They consist of a Lennard-Jones term, with parameters  $\epsilon_{ij}$  and  $\sigma_{ij}$ , and a Coulombic electrostatic term between partial charges  $q_i$ ,  $q_j$ . The dielectric constant  $\epsilon = \epsilon_0$ .  $\epsilon_r$  was set to  $\epsilon = \epsilon_0$ , i.e.,  $\epsilon_r = 1$ . Hydrogen bonds are described by the nonbonded terms in the energy function. In all of the calculations the long-range electrostatic terms were smoothly brought to zero at a cutoff of 12 Å by multiplication by a cubic switching function between 10 Å and 12 Å. Pairs of atoms on the same molecule separated by only two bonds may interact via a Urey-Bradley term harmonic in the distance between atoms  $i$  and  $j$ .

### Derivation of an adiabatic potential energy map

The Automatic Map Refinement Procedure (AMRP) was used to derive adiabatic potential energy maps for rotation about the C13=C14 and C15=N16 dihedral angles of retinal. This method, described in detail by Baudry et al. (1997), uses iterative energy minimizations in all of the wells in the potential energy surface examined. Smooth interpolation between the points obtained was performed using Akima's quintic polynomials implemented in the IDL package.

### Free energy calculations on retinal in bR

The goal of the free energy calculations was to compute the free energy difference between the two conformers in question. In theory this is independent of the pathway between them. However, the pathway is important in practice, as it influences the statistical accuracy of the calculations. In the present work we performed umbrella sampling along the "bicycle-pedal" pathway (Warshel, 1976), defined as  $\phi_1 = -\phi_2$ , where  $\phi_1$  is the C12-C13=C14-C15 dihedral and  $\phi_2$  is that of C14-C15=N16-C $\epsilon$ . This pathway was chosen because it preserves the direction of the retinal chain and is accompanied by only a small change in its shape, thus minimizing the environmental perturbation at each step. It has been suggested to be the pathway taken by retinal in bR during dark adaptation (Orlandi and Schulten, 1979; Tavan et al., 1985; Seltzer, 1987; Logunov and Schulten, 1996).

The starting structure for the MD free energy calculations on these molecules was obtained from Roux et al. (1996), based on the crystallographic structure of Grigorieff et al. (1996). Water molecules buried in the protein were placed according to thermodynamic criteria (Nina et al., 1995; Roux et al. 1996). These essentially reproduce the hydration patterns suggested by the newer x-ray crystallographic analyses of Pebay-Peyroula et al. (1997) and Luecke et al. (1998). Asp<sup>85</sup> is involved in hydrogen bonds

with two water molecules that are in very good agreement with those of the model of Luecke et al. (1998). Moreover, Pebay-Peyroula et al. suggest that four water molecules may lie between Asp<sup>96</sup> and the retinal, as in the model of Roux et al. (1996). However, we have repeated the basic conformational equilibrium calculation discussed in the present paper on the wild-type bR with the newer structure of Pebay-Peyroula et al. (1997). The result obtained was very similar to that obtained with the older, electron crystallographic structure.

To investigate the protein-retinal or water-retinal interactions, five systems were studied, four of which include some modification of the wild-type:

Wild-type bR, including five water molecules placed by Roux et al. (1996), i.e., four water molecules in the channel between H15 and Asp<sup>96</sup>, and a water near the Schiff base forming a hydrogen bond between the Schiff base, Asp<sup>85</sup> and Asp<sup>212</sup>. We call this “hydrated” bR.

A bR in which these five water molecules close to the Schiff base are removed (called here the “dehydrated retinal binding site”).

A bR in which Asp<sup>85</sup> is mutated to Ala (called “D85A”).

A bR in which Asp<sup>212</sup> is mutated to Ala (called “D212A”).

A bR in which both Asp<sup>85</sup> and Asp<sup>212</sup> are mutated to Ala (called here the “double mutant”).

The retinal force field of Nina et al. (1995), modified as in Baudry et al. (1997), was used in the MD calculations to evaluate the ((13,15)*cis*-all-*trans*) potential energy and free energy differences. For the protein part, version 22 of the CHARMM force field was used (MacKerell et al., 1998). The umbrella sampling method of Valleau and Torrie (1977) was used to calculate the two-dimensional potential of mean force (PMF) along  $\phi_1$  and  $\phi_2$ . In this method,  $N_w$  biased distributions are generated using harmonic functions of the form

$$w_i(\phi_1, \phi_2) = \frac{1}{2} K_1(\phi_1 - \phi_1^i)^2 + K_2(\phi_2 - \phi_2^i)^2 \quad (2)$$

centered on successive values of  $\phi_1^i$  and  $\phi_2^i$ . The umbrella sampled distributions were analyzed using the Weighted Histogram Analysis Method (WHAM) (Kumar et al., 1992), which has been extended to calculations along more than one degree of freedom (Roux, 1995). The WHAM equations express the optimal estimate for the unbiased distribution function as a weighted sum over the  $N_w$  individual biased distribution functions (Kumar et al., 1992; Roux, 1995) In the case of two variables,  $\phi_1$  and  $\phi_2$ , if  $n_i$  is the number of independent data points used to construct each biased distribution function, we have (Roux, 1995)

$$\langle \rho(\phi_1, \phi_2) \rangle = \sum_{i=1}^{N_w} n_i \langle \rho(\phi_1, \phi_2) \rangle_i \left[ \sum_{j=1}^{N_w} n_j e^{-(w_j(\phi_1, \phi_2) - F_j)/k_B T} \right]^{-1} \quad (3)$$

In Eq. 3,  $\rho(\phi_1, \phi_2)$  is the distribution function of the dihedral angles  $\phi_1$ ,  $\phi_2$ , and  $w_i$  and  $w_j$  are the harmonic restraint potentials used in umbrella sampling, where  $i$  and  $j$  denote the two constrained degrees of freedom. The undetermined constants  $F_j$  are defined from

$$e^{-F_j/k_B T} = \iint d\phi_1 d\phi_2 e^{-(w_j(\phi_1, \phi_2) - F_j)/k_B T} \langle \rho(\phi_1, \phi_2) \rangle \quad (4)$$

Because the distribution function itself depends on the set of constants  $F_j$ , the WHAM equations 3 and 4 must be solved self-consistently. In practice this is achieved through an iterative procedure. Self-consistency was typically reached after 2500 iterations, corresponding to a maximum change in  $F_j$  of  $2 \times 10^{-4}$  kcal/mol between successive iterations. The PMF,  $W(\xi)$  along a coordinate  $\xi = (\phi_1, \phi_2)$ , is defined from the average distribution function  $\langle \rho(\xi) \rangle$ :

$$W(\xi) = W(\xi^*) - k_B T \ln \left[ \frac{\langle \rho(\xi) \rangle}{\langle \rho(\xi^*) \rangle} \right] \quad (5)$$

where  $\xi^*$  and  $W(\xi^*)$  are arbitrary constants. The version of WHAM used takes advantage of the periodicity of the reaction coordinate to remove hysteresis.

The potential of mean force was calculated for  $\phi_1 (= -\phi_2)$  varying from  $+180^\circ$  to  $-180^\circ$  in steps of  $30^\circ$ , using the following protocol:

Step i.  $\phi_1$  and  $\phi_2$  were restrained to the desired values (i.e.,  $\phi_1 = 180^\circ$ ,  $\phi_2 = -180^\circ$ ;  $\phi_1 = 150^\circ$ ,  $\phi_2 = -150^\circ$ ; ...;  $\phi_1 = -180^\circ$ ,  $\phi_2 = 180^\circ$ ) with a force constant of 15 kcal/mol/degree<sup>2</sup>, giving a total of 13 windows of simulation.

Step ii. A 1-ps equilibration run was performed.

Step iii. Langevin production dynamics runs were performed, using the Langevin parameters listed in Roux et al. (1996).

For the simulations on mutated bR (i.e., mutations D85A, D212A, double mutant) and dehydrated binding-site bR, the time lengths were 20 ps per production window, giving a total production time of 260 ps for each modified protein. For the simulations on wild-type, hydrated bR, two simulations were performed:

A simulation with  $\phi_1$  varying from  $+180^\circ$  to  $-180^\circ$ , for which the production runs were performed for 18 ps. An additional 18-ps production run was performed in a window centered on  $\phi_1 = 160^\circ$ ,  $\phi_2 = -160^\circ$  to increase the sampling on this part of the diagonal, over which the free energy was found to have a relatively steep gradient. The total production time was 252 ps. This simulation is called the “forward” simulation.

A simulation with  $\phi_1$  varying from  $-180^\circ$  to  $+180^\circ$ , for which the production runs were 20 ps long. The total production time was thus 260 ps. This simulation is called the “backward” simulation.

For all of the simulations the potentials of mean force were calculated with 81 bins of width  $5^\circ$  for values of  $\phi_1$  and  $\phi_2$ , ranging from  $+202.5^\circ$  to  $-202.5^\circ$ . For the simulations on wild-type, hydrated bR, the potential of mean force was calculated from the forward and backward simulations independently, and from the combined umbrella-sampled distributions from both the forward and backward simulations, which is equivalent to a production time of 512 ps.

## RESULTS AND DISCUSSION

### Wild-type bacteriorhodopsin

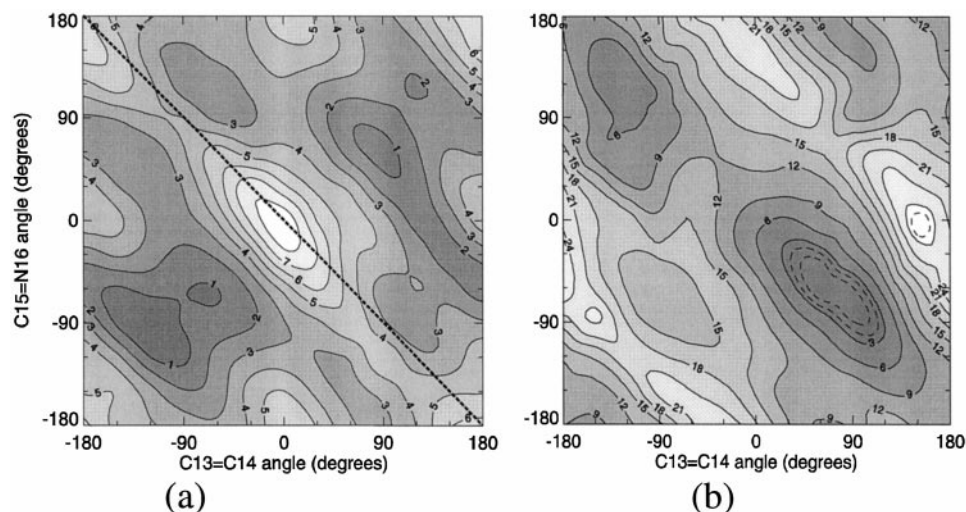
#### Isomerization pathway

We first examine possible isomerization pathways for the (13,15)*cis* to all-*trans* transition. This is done using adiabatic potential maps as a function of  $\phi_1$  and  $\phi_2$  in which all other degrees of freedom are relaxed. To aid in interpretation, we separate the potential energy into two components, the  $V_\phi$  twofold sinusoidal intrinsic torsional terms for  $\phi_1$  and  $\phi_2$  in Eq. 1, and the other terms, which we collectively label here the “environment.” The environment can include retinal-retinal, protein-retinal, and protein-protein interactions.

Fig. 2, *a* and *b*, show adiabatic potential energy maps for retinal isolated and in wild-type bR, respectively. These maps were calculated with the twofold intrinsic dihedral terms for  $\phi_1$  and  $\phi_2$  set to zero and thus provide an indication of the contribution of the environment to the rotational potential. The potential map for the retinal in bR shows larger variations than for isolated retinal, reflecting the presence of an explicit protein environment. In Fig. 2 *b* the diagonal corresponding to the bicycle pedal pathway is the lowest-energy pathway for all-*trans* to (13,15)*cis* conversion (i.e., going from  $\phi_1 = 180^\circ$ ,  $\phi_2 = 180^\circ$  to  $\phi_1 = 0^\circ$ ,  $\phi_2 = 0^\circ$ ).

The complete rotational map is given by the sum of the environmental contribution (in Fig. 2, *a* and *b*) and the

FIGURE 2 Adiabatic potential energy map for rotation around C13=C14 ( $\phi_1$ ) and C15=N16 ( $\phi_2$ ). (a) In vacuo retinal (Baudry et al., 1997), calculated with the parameters of Table 1, set B. The dashed line indicates the bicycle-pedal diagonal. (b) Retinal in bR, calculated with the parameters of Table 1, set B.



intrinsic terms. However, the values of the force constants for the intrinsic torsional terms are not known accurately. Although the torsional terms are difficult to derive directly from quantum chemistry, they can be expected to dominate quantum-mechanical rotational potentials of isolated polyene molecules. Semiempirical quantum-chemical calculations, using the modified neglect of diatomic overlap (MNDO) method on a retinal model without the  $\beta$ -ionone cycle and truncated after  $C_e$ , gave isomerization barriers of 13.7 kcal/mol and 21.5 kcal/mol for rotation around C13=C14 and C15=N16, respectively (Orlandi and Schulten, 1979). The isomerization barriers and the effect of negative fluoride ions near the retinal were subsequently studied with the modified neglect of diatomic overlap correlation (MNDOC) method (Tavan et al., 1985). Depending on the existence and position of the ions, the C13=C14 torsional barrier varied between 6.3 and 46.0 kcal/mol. The barrier along the bicycle-pedal pathway has been calculated using the modified neglect of diatomic overlap (MNDO) method with and without a negative ion located near the retinal (Seltzer, 1987). Without the ion, the energy barrier corresponding to a bicycle-pedal mechanism was found to be 24.6 kcal/mol. A negative ion located near the N16 atom of the Schiff base increased the barrier to 62.2 kcal/mol. In contrast, a ion located near the C13 carbon decreased the barrier to 15.2 kcal/mol. The above results suggest that the intrinsic barrier heights might be sensitive to the electrostatic environment of the retinal.

Protonation of Asp<sup>85</sup> is believed to be transient and to catalyze dark adaptation by lowering the free energy barrier between the all-*trans* and double-*cis* species (Balashov et al., 1995, 1996). Transient protonation of Asp<sup>85</sup> cannot change the equilibrium population (the *cis-trans* free energy difference). However, it might affect the pathway for conformational change and the associated potential energy barriers. In the present pathway calculations part of this effect is approximately included in the "intrinsic torsional term," which can include the effect of direct retinal polarization change induced by protonation.

In recent molecular dynamics studies, the intrinsic torsional barrier for C13=C14 was set to values ranging from 20.0 kcal/mol (Humphrey et al., 1994) to 25.8 kcal/mol (Hermone and Kuczera, 1998), whereas the C15=N16 double bond was set to values of 20.0 kcal/mol (Humphrey et al., 1994) to 30 kcal/mol (Nina et al., 1995), i.e., corresponding approximately to average values among those calculated from semiempirical methods. Nevertheless, the above considerations suggest that there is considerable uncertainty about the optimal values of  $k_{\phi}$  in Eq. 1 for the  $\phi_1$  (i.e., C13=C14) and  $\phi_2$  (i.e., C15=N16) torsions.

We find that the pathway of isomerization depends critically on the values chosen for  $k_{\phi_1}$  and  $k_{\phi_2}$ . Use of the intrinsic dihedral potential of Table 1, set A (i.e.,  $k_{\phi_1} = 3.15$  kcal/mol and  $k_{\phi_2} = 3.55$  kcal/mol, i.e., with intrinsic bar-

TABLE 1 Dihedral angle C13=C14 and C15=N16 force-field parameters

		$k_{\phi}$ (kcal/mol)	$n$	$\delta$ (degrees)
Set A	X—C13=C14—X	3.15*	2	180
	C12—C13=C14—C15	0.65	1	0
	X—C15=N16—X	3.55*	2	180
	C14—C15=N16—C $\epsilon$	0.51	1	180
	$R_{\min}$		$E_{\min}$	-0.11
Set B	X—C13=C14—X	0.00	2	180
	C12—C13=C14—C15	0.65	1	0
	X—C15=N16—X	0.00	2	180
	C14—C15=N16—C $\epsilon$	0.51	1	180
	$R_{\min}$		$E_{\min}$	-0.11

In CHARMM notation. Set A: Parameters used to compute the  $\Delta A$  values of Table 2. Set B: Parameters with zero intrinsic dihedral terms. X means any atom type. Four terms with periodicity  $n = 2$  and one with periodicity  $n = 1$  contribute to the intrinsic torsional energy.  $R_{\min}$  (in Å) is the van der Waals radius of the 1-4 vicinal  $sp^2$  carbon atoms (i.e., atom type CR\* in CHARMM (Nina et al., 1995), and  $E_{\min}$  (in kcal/mol) is the depth of the corresponding potential energy well.

\*From Humphrey et al. (1995).

riers of  $\sim 25$  kcal/mol for  $\phi_1$  and of  $\sim 28$  kcal/mol for  $\phi_2$ ) gives the adiabatic map in Fig. 3 *a*. This map is dominated by twofold cosine functions. The (13,15)*cis* ( $\phi_1 = 0^\circ$ ,  $\phi_2 = -5^\circ$ ) structure is the global minimum of the map. The all-*trans* ( $\phi_1 = 180^\circ$ ,  $\phi_2 = 180^\circ$ ) structure is in a local minimum, 2.1 kcal/mol higher than (13,15)*cis*. The bicycle pedal is not the lowest energy pathway here, which corresponds to a sequential isomerization of the two dihedral angles with a barrier of  $\sim 34$  kcal/mol. A situation in which two alternative pathways can be sampled was found by lowering the intrinsic dihedral force constants,  $k_{\phi_1}$  and  $k_{\phi_2}$ , to 1.88 kcal/mol, i.e., with intrinsic barriers of  $\sim 15$  kcal/mol. This gives the adiabatic map in Fig. 3 *b*. The two low-energy pathways, A and B, have potential energy barriers of  $\sim 22$  kcal/mol each, equal to a value proposed in the previous quantum-chemical study of dark adaptation in bR (Logunov and Schulten, 1996). This potential energy barrier was calculated by Logunov and Schulten along the bicycle-pedal pathway with Asp<sup>85</sup> protonated. Transient protonation of Asp<sup>85</sup> is suggested to catalyze the dark adaptation of bR (Balashov et al., 1995, 1996) by lowering the free-energy barrier along the transition pathway. Thus the adiabatic map in Fig. 3 *b* is obtained with a barrier that corresponds to the case of Asp<sup>85</sup> protonated. Path A in Fig. 3 *b* is very close to the bicycle-pedal mechanism, whereas path B involves sequential rotations of the  $\phi_1$  (i.e., C13=C14) and  $\phi_2$  (i.e., C15=N16) dihedral angles, as in the case of Fig. 3 *a*. Further reduction of  $k_{\phi_1}$  and  $k_{\phi_2}$  leads to the bicycle pedal pathway being that with the lowest barrier.

#### Decomposition of the (13,15)-all-*trans* potential energy difference

The structures obtained from the adiabatic maps were used to decompose the potential energy difference between the

(13,15)*cis* and all-*trans* species in the protein. Calculation of the energy difference including only the Lys<sup>216</sup>-retinal atoms in Fig. 1 gives an energy for all-*trans* 1.7 kcal/mol lower than that for (13,15)*cis*. This value is not far from the value of 2.1 kcal/mol found for the isolated retinal molecule. The energy difference for bR not including the Lys<sup>216</sup>-retinal atoms is, in contrast, 3.9 kcal/mol in favor of the (13,15)*cis* form. In contrast, the difference in the remaining energy, the interaction between the LYR moiety and the rest of the protein, is only  $\sim 0.1$  kcal/mol. These calculations indicate that the presence of the protein stabilizes the (13,15)*cis* retinal form relative to all-*trans*, and that this stabilization results from improved protein-protein interactions in the (13,15)*cis* species, rather than protein-retinal or retinal-retinal interactions. Decomposition of the protein-protein interactions themselves showed that they contain many small contributions.

The low value of the interaction energy between LYR and the rest of the protein is due to cancellation between relatively large contributions. In particular, the deprotonated residue Asp<sup>212</sup> was found to stabilize the (13,15)*cis* form by  $\sim 9$  kcal/mol, whereas in contrast, the water molecules placed by Roux et al. (1996) in the retinal binding site have the opposite effect, stabilizing the all-*trans* form by  $\sim 4$  kcal/mol. Asp<sup>85</sup> was found not to strongly influence the potential energy difference. These results indicate that removal of buried water molecules or of the Asp<sup>212</sup> residue near the Schiff base might have significant effects on the conformational equilibrium. These possibilities are further examined below in free energy calculations.

#### Potential of mean force along the bicycle-pedal pathway

The umbrella sampling method was used to calculate a potential of mean force,  $\Delta A$ , along the bicycle-pedal path-

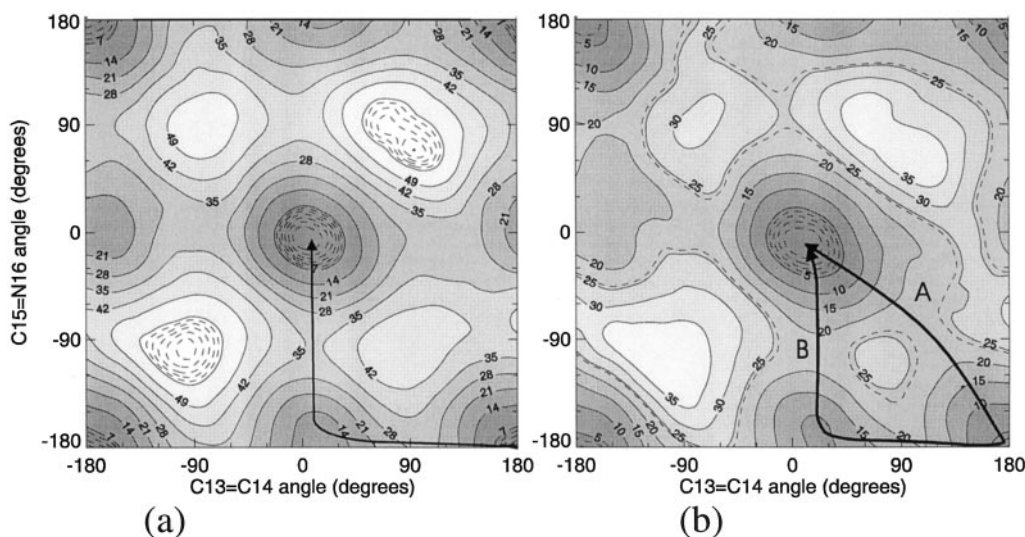


FIGURE 3 Adiabatic potential energy map for rotation around C13=C14 ( $\phi_1$ ) and C15=N16 ( $\phi_2$ ) retinal in bR. (a) Calculated with the parameters of Table 1, set A. The arrow indicates the lowest energy pathway for *trans* to *cis* isomerization of the two double bonds. (b) Calculated with the intrinsic dihedral force constants of 1.88 kcal/mol for these dihedrals. Arrows indicate the lowest energy pathways for *trans* to *cis* isomerization of the two double bonds.

way, as described in Methods. Fig. 4 *a* shows the calculated free energy surface in the protein with the use of the potential energy function of Table 1, set B. In this set, the twofold dihedral terms for the C13=C14 and C15=N16 angles are zero. Two minima are seen, at  $\phi_1 = +70^\circ$  and  $-110^\circ$ , the former being the lowest. The maximum of the surface is located at  $\phi_1 = +130^\circ$  and is  $\sim 10$  kcal/mol above the minimum. The corresponding bicycle-pedal diagonal for the isolated retinal model is shown in Fig. 4 *b*. The maxima and minima of this diagonal are similar to those of the potential energy map in Fig. 2 *a*. However, the maximum in the free energy profile along the bicycle-pedal diagonal is two times higher in the protein than for the isolated retinal. Use of the potential of Table 1, set A, i.e., including the intrinsic torsional terms, gives the free energy surface shown in Fig. 4 *c*. The minima here are located at  $(\phi_1 = 185^\circ, \phi_2 = -180^\circ)$  and  $(\phi_1 = 5^\circ, \phi_2 = -5^\circ)$ , the latter being the lower. These two minima correspond to the all-*trans* and (13,15)*cis* forms of retinal, respectively.

The free energy surface in Fig. 4 *c* is calculated to provide a means of estimating the free energy difference ( $\Delta A$ ) between the conformers. The free energy barrier between the two equilibrium species, although important for the rate of the transition, is not necessarily meaningful in our calculations, because of the errors and uncertainties of the method. Table 2 gives the values of the calculated (13,15)*cis*-all-*trans* free energy for the different systems examined. For the forward and backward simulations of wild-type, hydrated bR, the calculated (13,15)*cis*-all-*trans* free energy differences  $\Delta A$  are  $-1.6$  kcal/mol and  $-1.2$  kcal/mol, respectively, the (13,15) species being the more stable. When the umbrella-sampled distributions of the forward and backward simulations are merged together and unbiased with WHAM, the ((13,15)*cis*-all-*trans*)  $\Delta A$  is  $-1.1$  kcal/mol. This value is close to the  $\Delta A$  calculated from the backward simulation. In comparison, the experimentally observed population ratio of 67% (13,15)*cis* and 33% all-*trans* at 300 K corresponds to a free energy difference of  $-0.5$  kcal/mol between the two species, the (13,15)*cis* species being the more stable. These results contrast with the calculations on isolated retinal for which the calculated  $\Delta A$  is 2.1 kcal/mol in favor of the all-*trans* species.

### Modified bacteriorhodopsin

Calculations were performed of the (13,15)*cis*-all-*trans* free energy difference for the modified bR structures described in Methods. The results are summarized in Table 2.

The interaction energy calculations discussed above (under Wild-Type Bacteriorhodopsin) suggest that internal water molecules might stabilize the all-*trans* conformer in the protein. To determine if this result is also true in free energy terms, the (13,15)*cis*-all-*trans* free energy difference for dehydrated binding-site bR, with the internal water molecules removed from retinal binding pocket, was calculated. This led to the (13,15)*cis* being the form of lowest free

energy, as in the hydrated wild type. However, the free energy of the the all-*trans*, dehydrated retinal binding pocket species was found to be 4.2 kcal/mol higher than the (13,15)*cis* species (1.1 kcal/mol in the case of the hydrated species). Therefore these calculations confirm the stabilization of the all-*trans* species by the internal buried water molecules in bR. Experimental dehydration has been shown to destabilize the all-*trans* chromophore (Korenstein and Hess, 1977). However, the water molecules removed in the present calculations are the five water molecules placed by Roux et al. (1996) between residues Asp<sup>96</sup> and Asp<sup>85</sup>. This dehydration probably does not correspond to that experimentally performed (Zaccai, 1987; Ferrand et al., 1993a; Lehnert et al., 1998), in which the water molecules removed by dehydration are mainly localized around the lipid headgroups. The dehydration simulated here corresponds to a selective dehydration of the core of bR, in the retinal binding site.

The interaction energy calculations also suggested that the effect of Asp<sup>212</sup> might be to stabilize the (13,15)*cis* isomer, the opposite of the effect of the water molecules. The calculation of  $\Delta A$  for the D212A mutant led to the all-*trans* species being 0.8 kcal/mol lower in free energy than the (13,15)*cis* species. This result again concurs with the interaction energy calculations, in that Asp<sup>212</sup> significantly stabilizes the (13,15)*cis* isomer.

The interaction energies showed no significant influence of the Asp<sup>85</sup> residue on the *cis-trans* interaction energy difference. This was also found for the calculations of  $\Delta A$  for the D85A mutant, which gave the result that the (13,15)*cis* species is 1.6 kcal/mol lower in free energy than the all-*trans* species. This  $\Delta A$  is not significantly different from the wild type, again in accord with the interaction energy calculations. There is experimental evidence that the protonation of Asp<sup>85</sup> affects the equilibrium, although not very strongly (Fischer and Oesterhelt, 1979; Turner et al., 1993; Balashov et al., 1996). However, the accuracy of the present free energy calculations is certainly not better than  $k_B T$ , and consequently only large population changes are amenable to investigation by simulation techniques.

Finally, to investigate the effect of complete removal of the negative charge around the Schiff base, free energy calculations were performed on the double mutant D85A and D212A. The (13,15)*cis*-all-*trans* free energy difference obtained was 1.9 kcal/mol, the all-*trans* species being the more stable, as in the case of the single mutation D212A. This result suggests that mutation of these aspartic acids to alanine, which renders impossible the formation of hydrogen bonds between retinal and these side chains, leads to a stabilization of the all-*trans* species.

Table 2 also gives the (13,15)*cis*-all-*trans* adiabatic potential energy differences ( $\Delta E$ ) for the above molecular systems. The values of  $\Delta E$  and  $\Delta A$  are generally quite close, with a maximum difference of  $\sim 1$  kcal/mol. This suggests that the calculated free energy differences are essentially enthalpic.

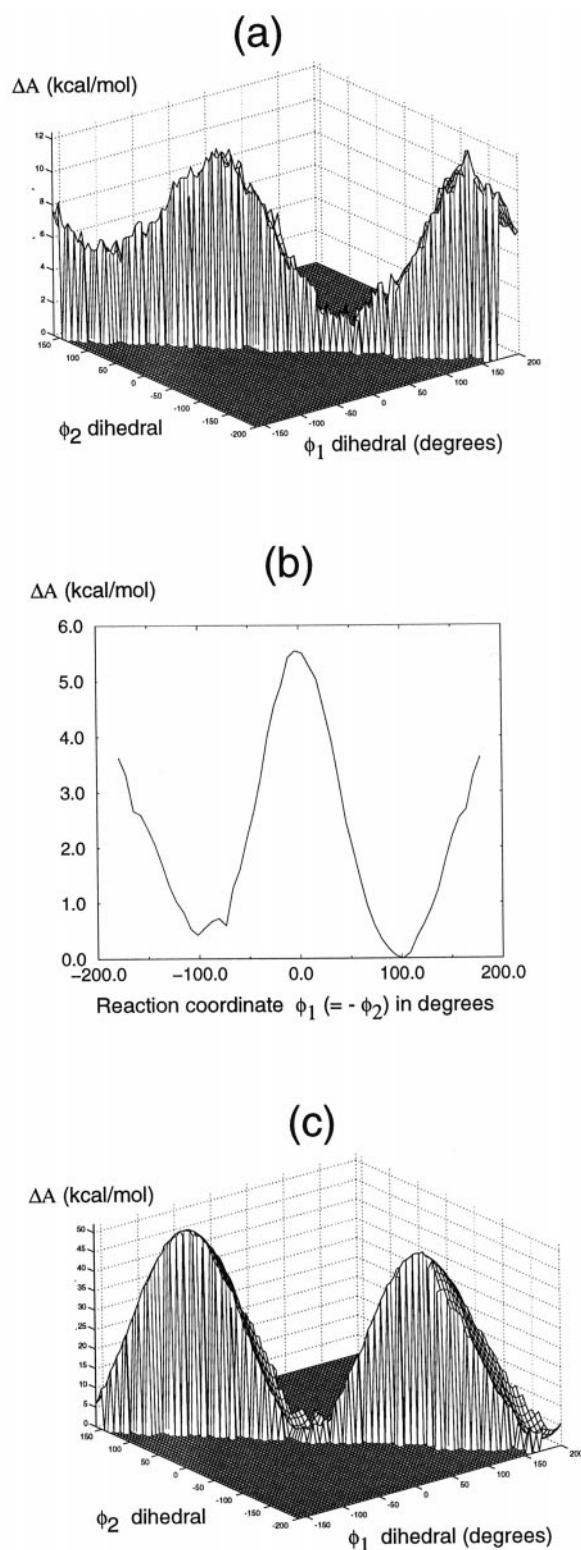


FIGURE 4 (a) Free energy surface along the bicycle-pedal diagonal, calculated with the parameters of Table 1, set B. The 22 kcal/mol energy contour is represented by a dashed line. (b) Free energy profile along the bicycle-pedal diagonal for retinal in vacuo constrained to have the same (all-*trans*) average structure as retinal in bR (see Baudry et al., 1997). Only the portion of the two-dimensional free energy map corresponding to the strict diagonal-pedal (i.e.,  $\phi_1 = \phi_2$ ) is shown here, to facilitate the comparison with a. (c) Free energy surface along the bicycle-pedal diagonal, calculated with the parameters of Table 1, set A.

TABLE 2 Free energy ( $\Delta A$ ) and potential energy ( $\Delta E$ ) differences

	$\Delta A$ [(13,15) <i>cis</i> -all- <i>trans</i> ]	$\Delta E$ [(13,15) <i>cis</i> -all- <i>trans</i> ]
In vacuo retinal*	+2.1	+2.1
Wild-type, hydrated bR		-2.1
Forward simulation	-1.6	
Backward simulation	-1.2	
Forward + backward	-1.1	
Mutated or modified bR		
Dehydrated binding site	-4.2	-4.6
D85A	-1.6	-1.4
D212A	+0.8	+1.1
Double mutant D212A and D85A	+1.9	+1.3

\*From Baudry et al. (1997).

#### Structures of bR in the wild-type, hydrated protein

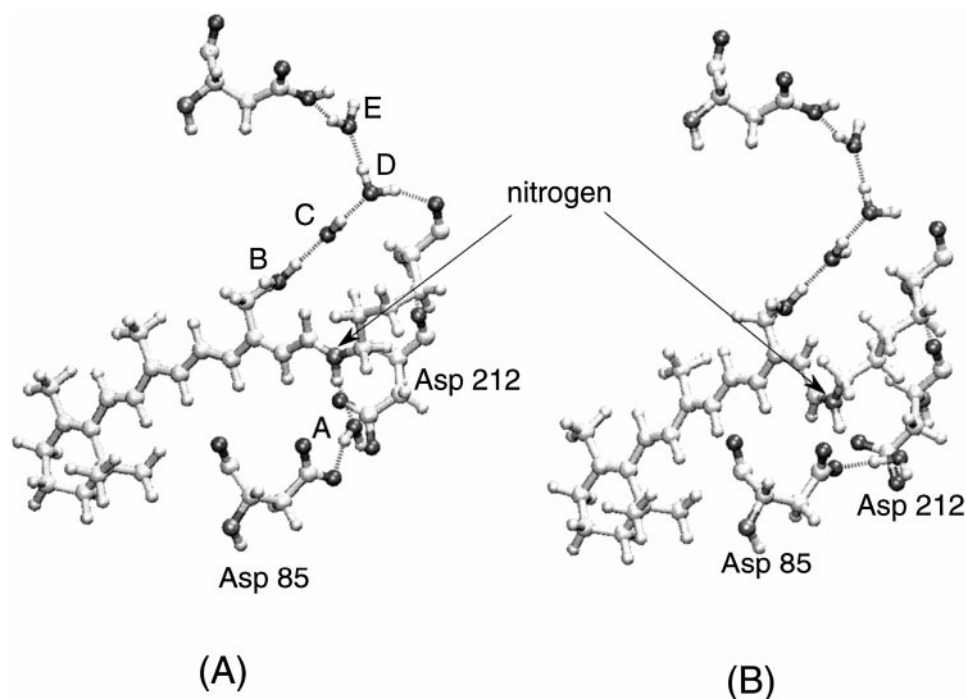
The structure of retinal in bR is shown in Fig. 5, *a* and *b*, for the all-*trans* and (13,15)*cis* species, respectively. The hydrogen-bonding network between the water molecules is essentially unaffected by the conformational transition. The planarity of the retinal is preserved in the (13,15)*cis* species, with the notable exception of a twist of the C13=C14-C15=N16 dihedral angle, from  $-179^\circ$  in the equilibrated all-*trans* structure to  $162^\circ$  in the equilibrated (13,15)*cis* structure. The presence of distortion in the retinal is in agreement with conclusions from solid-state NMR measurements, in which a  $^{13}\text{C}$  resonance of bR<sub>548</sub> that is shifted downfield compared to bR<sub>568</sub> was explained by a possible twist in the retinal chain in the C13=C14-C15 region (de Groot et al., 1989). This is also in agreement with resonance Raman spectra of bR<sub>548</sub> (Smith et al., 1989), which showed an intense out-of-plane vibration of the proton attached to C14 that was also interpreted as a distortion from the planar retinal structure.

#### CONCLUSIONS

The present work involved investigating factors influencing the (13,15)*cis*-all-*trans* conformational transition and thermodynamic equilibrium in dark-adapted bacteriorhodopsin. Errors in the calculated free energies are unlikely to be smaller than  $\sim k_B T$  (i.e., 0.6 kcal/mol at 300 K), even for long simulations on systems of a limited number of atoms (Baudry et al., 1997). Comparison of the wild-type hydrated bR free energy difference calculated from the forward, backward, and forward + backward simulations shows results that are in agreement with each other to within  $\sim k_B T$ . Moreover, our best estimate of the wild-type  $\Delta A$  of  $-1.1$  kcal/mol is also within  $\sim k_B T$  of experiment. Consequently, we consider the present results to be satisfactory, given the inherent limitations of the methods.

The calculations identify two groups of atoms that strongly influence the conformational equilibrium. The double mutation D85A/D212A modifies the free energy differ-

FIGURE 5 (a) Average structure of the retinal region in the all-*trans* form. Labels A–E for the water molecules are taken from Roux et al. (1996). (b) Average structure of the retinal region in the (13–15)*cis* form. This figure was made with the program VMD (Humphrey et al., 1996).



ence by  $\sim 3$  kcal/mol, in favor of the all-*trans* species. In contrast, removal of the internal water molecules stabilizes the (13,15)*cis* species by  $\sim 3$  kcal/mol. Thus the Asp residues located near the Schiff base and the internal water molecules have effects on the stability of the two species that are opposite but of similar magnitude. The present calculations suggest that the opposing actions of these two groups of atoms approximately cancel in wild-type bR, leading to a similar free energy of the two species to within  $\sim k_B T$ . The effects on the free energy difference of the protein modifications examined here are  $\sim 5k_B T$  and are likely to be above the error level. The results suggest that if it were possible experimentally to remove the internal water molecules, or to perform the double Asp  $\rightarrow$  Ala mutation, the *cis/trans* equilibrium should be measurably affected. To our knowledge, these experiments have not been yet performed.

The bR model used in this paper is a monomeric model of the protein, in which the average effect of the environment is simulated approximately by the use of weak harmonic restraints on the position of  $\alpha$ -carbons located at the surface of bR (Ferrand et al., 1993b; Roux et al., 1996). Repetition of the present calculations using a model including explicitly trimeric bR in a lipid bilayer would be of interest, although computationally expensive. However, it has been found that the 1:2 population ratio between the two conformers of retinal in dark-adapted bR remains on dissociation into monomeric bR (Scherrer et al., 1989; Song et al., 1995).

The pathway for conformational change from (13,15)*cis* to all-*trans* in dark-adapted bR is currently unknown. Our calculations separate the factors influencing the pathway into two: the intrinsic torsional term and the rest (the “en-

vironment”). Whereas the intrinsic terms favor sequential rotation, the environment favors a bicycle-pedal mechanism. We find that the lowest-energy pathway found depends critically on the balance between these effects. As quantum-chemical and molecular-mechanical calculations become more precise, it should be possible in the near future to use theory to help decide which of the two pathways is favored in bR.

We acknowledge support from NATO grant number 920093.

## REFERENCES

- Balashov, S. P., R. Govindjee, E. S. Imasheva, S. Misra, T. G. Ebrey, Y. Feng, R. K. Crouch, and D. R. Menick. 1995. The two pKa's of aspartate-85 and control of thermal isomerization and proton release in the arginine-82 to lysine mutant of bacteriorhodopsin. *Biochemistry*. 34:8820–8834.
- Balashov, S. P., E. S. Imasheva, R. Govindjee, and T. G. Ebrey. 1996. Titration of aspartate-82 in bacteriorhodopsin: what it says about chromophore isomerization and proton release. *Biophys. J.* 70:473–481.
- Baudry, J., S. Crouzy, B. Roux, and J. C. Smith. 1997. Quantum chemical and free energy simulation analysis of retinal conformational energetics. *J. Chem. Inf. Comput. Sci.* 37:1018–1024.
- Ben-Nun, M., F. Molnar, H. Lu, J. C. Phillips, T. J. Martínez, and K. Schulten. 1998. Quantum dynamics of retinal's femtosecond photoisomerization in bacteriorhodopsin. Chemical reaction theory. Special issue. *Faraday Discuss.* 110:447.
- Brooks, B. R., R. E. Bruccoleri, B. D. Olafson, D. J. States, S. Swaminathan, and M. Karplus. 1983. CHARMM: a program for macromolecular energy minimization and dynamics calculations. *J. Comp. Chem.* 4:187–217.
- de Groot, H. J. M., G. S. Harbison, J. Herzfeld, and R. G. Griffin. 1989. Nuclear magnetic resonance study of the Schiff base in bacteriorhodopsin counterion effects on the  $^{15}\text{N}$  shift anisotropy. *Biochemistry*. 28:3346–3353.

- Edholm, O., O. Berger, and F. Jähnig. 1995. Structure and fluctuations of bacteriorhodopsin in the purple membrane: a molecular dynamics study. *J. Mol. Biol.* 250:94–111.
- Ferrand, M., A. J. Dianoux, W. Petry, and G. Zaccaï. 1993a. Thermal motions and function of bacteriorhodopsin in purple membrane: effects of temperature and dehydration studied by neutron scattering. *Proc. Natl. Acad. Sci. USA.* 90:9668–9672.
- Ferrand, M., G. Zaccaï, M. Nina, J. C. Smith, C. Etchebest, and B. Roux. 1993b. Structure and dynamics of bacteriorhodopsin: comparison of simulation and experiment. *FEBS Lett.* 327:256–260.
- Fischer, U., and D. Oesterhelt. 1979. Chromophore equilibrium in bacteriorhodopsin. *Biophys. J.* 28:211–230.
- Grigorieff, T. A., K. H. Ceska, K. H. Downing, J. M. Baldwin, and R. Henderson. 1996. Electron-crystallographic refinement of the structure of bacteriorhodopsin. *J. Mol. Biol.* 259:393–421.
- Harbison, G. S., S. O. Smith, J. A. Pardo, C. Winkel, J. Lugtenberg, J. Herzfeld, R. Mathies, and R. G. Griffin. 1984. Dark-adapted bacteriorhodopsin contains 13-*cis*,15-*syn* and all-*trans*,15-*anti* retinal Schiff bases. *Proc. Natl. Acad. Sci. USA.* 81:1706–1709.
- Hermone, A., and K. Kuczera. 1998. Free-energy simulations of the retinal *cis* → *trans* isomerization in bacteriorhodopsin. *Biochemistry.* 37:2843–2853.
- Humphrey, W., A. Dalke, and K. Schulten. 1996. VMD—visual molecular dynamics. *J. Mol. Graph.* 14:33–38.
- Humphrey, W., I. Logunov, K. Schulten, and M. Sheves. 1994. Molecular dynamics study of bacteriorhodopsin and artificial pigments. *Biochemistry.* 33:3668–3678.
- Humphrey, W., H. Lu, I. Logunov, H. J. Werner, and K. Schulten. 1998. Three electronic state model of the primary phototransformation of bacteriorhodopsin. *Biophys. J.* 75:1689–1699.
- Korenstein, R., and B. Hess. 1977. Hydration effects on the photocycle of bacteriorhodopsin in thin layers of purple membrane. *Nature.* 270:184–186.
- Kumar, S., D. Bouzida, R. H. Swendsen, P. A. Kollman, and J. M. Rosenberg. 1992. The weighted histogram analysis method for free-energy calculations on biomolecules. I. The method. *J. Comp. Chem.* 13:1011–1021.
- Lehnert, U., V. Réat, M. Weik, G. Zaccaï, and C. Pfister. 1998. Thermal motions in bacteriorhodopsin at different hydration levels studied by neutron scattering: correlation with kinetics and light-induced conformational changes. *Biophys. J.* 75:1945–1952.
- Logunov, I., W. Humphrey, K. Schulten, and M. Sheves. 1995. Molecular dynamics study of the 13-*cis* form ( $\text{br}_{548}$ ) of bacteriorhodopsin and its photocycle. *Biophys. J.* 68:1270–1282.
- Logunov, I., and K. Schulten. 1996. Quantum chemistry: molecular dynamics study of the dark-adaptation process in bacteriorhodopsin. *J. Am. Chem. Soc.* 118:9727–9735.
- Luecke, H., H. T. Richter, and J. K. Lanyi. 1998. Proton transfer pathways in bacteriorhodopsin at 2.3 Å resolution. *Science.* 280:1934–1937.
- MacKerell, A. D., Jr., D. Bashford, M. Bellot, R. L. Dunbrack, Jr., J. D. Evaseck, M. J. Field, S. Fisher, J. Gao, H. Guo, S. Ha, D. Joseph-McCarthy, L. Kuchnir, K. Kuczera, F. T. K. Lau, C. Mattos, S. Michnik, T. Ngo, D. T. Nguyen, B. Prodhom, W. E. Reiher, III, B. Roux, M. Schlenkrich, J. C. Smith, R. Stote, J. Straub, M. Watanabe, J. Wiorkiewicz-Kuczera, D. Yin, and M. Karplus. 1998. All-atom empirical potential for molecular modeling and dynamics studies of proteins. *J. Phys. Chem. B.* 102(18):3586–3616.
- Massote, D., and J. Aghion. 1991. Bacteriorhodopsin “detergent-monomers” blue shift and velocity of light-dark-adapted adaptation. *Biochem. Biophys. Res. Commun.* 181:1301–1305.
- Nina, M., B. Roux, and J. C. Smith. 1995. Functional interactions in bacteriorhodopsin: a theoretical analysis of retinal hydrogen bonding with water. *Biophys. J.* 68:25–39.
- Nina, M., J. C. Smith, and B. Roux. 1993. Ab-initio quantum chemical analysis of Schiff base-water interactions in bacteriorhodopsin. *J. Mol. Struct. (Theochem).* 286:231–245.
- Oesterhelt, D., and W. Stoekenius. 1971. Rhodopsin-like protein from the purple membrane of *Halobacterium salinarum*. *Nature New Biol.* 233:149–152.
- Orlandi, G., and K. Schulten. 1979. Coupling of stereochemistry and proton donor-acceptor properties of a Schiff base. A model of a light-driven proton pump. *Chem. Phys. Lett.* 64:370–374.
- Pebay-Peyroula, E., G. Rummel, J. P. Rosenbuch, and E. M. Landau. 1997. X-ray structure of bacteriorhodopsin at 2.5 Å from microcrystal growth in lipidic cubic phases. *Science.* 277:1676–1691.
- Roux, B. 1995. The calculation of the potential of mean force using computer simulations. *Comput. Phys. Commun.* 91:275–282.
- Roux, B., M. Nina, R. Pomès, and J. C. Smith. 1996. Thermodynamic stability of water molecules in the bacteriorhodopsin proton channel: a molecular dynamics free energy perturbation study. *Biophys. J.* 71:670–681.
- Scherrer, P., M. K. Mathew, W. Sperling, and W. Stoekenius. 1989. Retinal isomer ratio in dark-adapted purple membranes and bacteriorhodopsin monomer. *Biochemistry.* 28:829–834.
- Schulte, A., and L. Bradley, II. 1995. High pressure near-infrared Raman spectroscopy of bacteriorhodopsin light to dark adaptation. *Biophys. J.* 69:1554–1562.
- Schulte, A., L. Bradley, II, and C. Williams. 1995. Equilibrium composition of retinal isomer in dark-adapted bacteriorhodopsin and effect of high pressure probed by near-infrared Raman spectroscopy. *Appl. Spectrosc.* 49:80–83.
- Seltzer, S. 1987. MNDO barrier heights for catalyzed bicycle pedal, hula-twist, and ordinary *cis-trans* isomerizations of protonated retinal Schiff base. *J. Am. Chem. Soc.* 109:1627–1631.
- Smith, S. O., H. J. M. de Groot, R. Gebhard, J. M. L. Courtin, J. Lugtenberg, J. Herzfeld, and R. G. Griffin. 1989. Structure and protein environment of the retinal chromophore in light- and dark-adapted bacteriorhodopsin studied by solid-state NMR. *Biochemistry.* 28:8897–8904.
- Song, L., D. Yang, M. A. El-Sayed, and J. K. Lanyi. 1995. Retinal composition in some bacteriorhodopsin mutants under light and dark adaptation conditions. *J. Phys. Chem.* 99:10052–10055.
- Tavan, P., K. Schulten, and D. Oesterhelt. 1985. The effect of protonation and electrical interactions on the stereochemistry of retinal Schiff bases. *Biophys. J.* 47:415–430.
- Turner, G. J., L. J. W. Miercke, T. E. Thorgeirsson, D. S. Klinger, M. C. Betlach, and R. M. Stroud. 1993. Bacteriorhodopsin D85N three spectroscopic species in equilibrium. *Biochemistry.* 32:1332–1335.
- Valleau, J. P., and G. M. Torrie. 1977. A guide for Monte-Carlo for statistical mechanics. In *Statistical Mechanics, Part A*. B. J. Berne editor. Plenum Press, New York. 169–194.
- Warshel, A. 1976. Bicycle-pedal model for the first step in the vision process. *Nature.* 260:679–683.
- Xu, D., C. Martin, and K. Schulten. 1996. Molecular dynamics study of early picosecond events in the bacteriorhodopsin photocycle: dielectric response, vibrational cooling and the J, K intermediates. *Biophys. J.* 70:453–460.
- Xu, D., M. Sheves, and K. Schulten. 1995. Molecular dynamics study of the M412 intermediate of bacteriorhodopsin. *Biophys. J.* 69:2745–2760.
- Zaccaï, G. 1987. Structure and hydration in the purple membrane of *Halobacterium halobium*: a neutron diffraction study. *J. Mol. Biol.* 194:569–572.